Heliyon 10 (2024) e36324

Contents lists available at ScienceDirect

Heliyon

journal homepage: www.cell.com/heliyon

Research article

A cuproptosis-related prognostic signature for guiding clinical diagnosis and treatment in uveal melanoma patients

Ying Yang [a,c,1], Qixuan Li [b,c,1], Jia Chen [a], Yangchen Guo [c], Yu Cai [a,c], Wenmin Zhao [c,d], Shu Su [a,**], Aimin Sang [a,*]

[a] Eye Institute, Affiliated Hospital of Nantong University, Nantong, 226001, Jiangsu, China
[b] Department of Thoracic Surgery, Affiliated Hospital of Nantong University, Nantong, 226001, Jiangsu, China
[c] Medical School of Nantong University, Nantong, Jiangsu, China
[d] Department of Dermatology, Affiliated Hospital of Nantong University, Nantong, 226001, Jiangsu, China

ARTICLE INFO

Keywords:
Cuproptosis
Uveal melanoma (UM)
Prognostic signature
Immune microenvironment
DLD
DLST

ABSTRACT

Background: Cuproptosis, one of the most recently discovered forms of cell death, is induced by the disruption of copper binding to the mitochondrial respiratory acylation components. However, the mechanism underlying cuproptosis in uveal melanoma (UM) has not yet been adequately studied.

Methods: RNA and clinical data were obtained from The Cancer Genome Atlas (TCGA) database. Differentially expressed cuproptosis-related genes were identified by R software. A prognostic signature was constructed by applying LASSO regression and Cox regression models. The associations between the signature and the immune microenvironment, overall survival, and drug sensitivity were studied. In addition, qPCR and Western blotting were performed on UM cells and RPE cell lines to verify the expression levels of the genes encoding dihydrolipoamide dehydrogenase (DLD) and dihydrolipoamide S-succinyltransferase (DLST) in UM cases.

Results: Using a cuproptosis-related prognostic signature, UM samples were classified into high- and low-risk groups. A significant difference in overall survival between the two risk groups was evident. Receiver operating characteristic curves demonstrated that the signature is a reliable predictor of prognosis. Immune cell infiltration, drug sensitivity, and immune checkpoint expression were analysed. Significant immune difference between the two high-risk groups was found, and the high expression of immune checkpoints in high-risk groups suggests significant immunotherapy potential. In addition, drug sensitivity analysis experiments suggest that erlotinib may be a potential treatment for high-risk patients. The results of in vitro experiments confirmed that DLD and DLST had higher expression levels in UM cell lines.

Conclusions: The prognostic signature developed in this study is a reliable biomarker for predicting the prognosis of UM and may serve as a tool for personalised treatment of patients with UM.

* Corresponding author.
** Corresponding author. Department of Ophthalmology, Affiliated Hospital of Nantong University, Nantong, 226001, Jiangsu, China.
E-mail addresses: sushu.sunny@aliyun.com (S. Su), sangam@ntu.edu.cn (A. Sang).
[1] These authors contributed equally to this work.

https://doi.org/10.1016/j.heliyon.2024.e36324
Received 5 August 2023; Received in revised form 13 August 2024; Accepted 13 August 2024
Available online 14 August 2024

1. Introduction

Uveal melanoma is a melanoma located in the choroid, ciliary body, and iris of the eye [1,2]. It is an invasive malignant tumour originating from melanocytes in the eyes [3]. UM is the most common primary intraocular tumour in adults, with an age-adjusted average incidence rate of 5.1 cases per million per year [4]. After the primary tumour is successfully treated with radiotherapy or surgery, approximately 50 % of UM patients eventually develop metastatic disease and die of metastasis within 10 years of diagnosis [3,5].

Over the years, with advances in treatment strategies, the rate of local tumour control and global salvage rate have improved. However, survival rates have remained relatively constant [6]. With the development of new therapies, tracking treatment and survival rates of patients with uveal melanoma is becoming increasingly important. Therefore, there is an urgent need to identify new biomarkers that can be used to stratify UM cases and treat patients directly.

Copper, as one of the key elements in human physiological metabolism, is involved in numerous biological metabolic activities [7]. Copper has both positive and negative effects in the body, and even moderate intracellular concentrations can be toxic, leading to cell death [8]. Tsvetkov et al. discovered cuproptosis and provided a detailed explanation, showing that it occurs via the binding of fatty acylation components and copper in tricarboxylic acid (TCA) cycles [9]. This leads to the polymerisation of lipidic proteins and loss of iron-sulphur cluster proteins, which causes protein toxicity and ultimately cell death [9].

Tumor cells can decouple glycolysis and the TCA cycle, leading to the use of other fuel sources, such as glutamine, to meet their increased metabolic needs [10,11]. Increased glutamine metabolism promotes UM cell proliferation and metastasis [12]. Owing to the crucial role of copper in human physiology, cuproptosis has potential as a new approach to promoting tumour cell death [13]. Researchers have used these cuproptosis-related genes for bioinformatic analysis and have constructed prognostic signatures [14–16]. Given the recency of the research on cuproptosis, there is lack of information concerning the exact mechanism of cuproptosis in UM. Therefore, constructing a cuproptosis-related prognostic signature is meaningful for predicting prognosis and directing the treatment of patients with UM. In this study, we identified differentially expressed cuproptosis-related genes from The Cancer Genome Atlas (TCGA) database and constructed a prognostic signature based on these DEGs. The UM samples were divided into high- and low-risk subsets. Significant differences in overall survival (OS) were found between the two risk groups, and prognostic features have been shown to predict prognosis and provide new tools for personalised treatment of UM patients.

2. Materials and methods

2.1. Data capture and preprocessing

The mRNA sequence data and clinical information were obtained from the TCGA-UM dataset (https://portal.gdc.cancer.gov/). After eliminating unqualified mRNA sequences and clinical data, we obtained 80 UM patients. In addition, we downloaded the mRNA sequence data and clinical information from 61 patients with UM from the Gene Expression Omnibus (GEO) database GSE22138 dataset for independent validation of the stability of this prognostic signature.

2.2. Construction of the prognostic signature

Based on the overall survival data of patients with UM, obtained from the TCGA dataset, univariate Cox Regression analysis was applied to screen for cuproptosis-related genes. Applying the R package “glmnet”, LASSO Cox regression was conducted and four cuproptosis-related genes were found to be significantly associated with UM OS. Lastly, according to multivariate Cox regression analysis, the genes encoding dihydrolipoamide dehydrogenase (DLD) and dihydrolipoamide S-succinyltransferase (DLST) were identified as prognostic cuproptosis-related genes. The cuproptosis-related risk signature was established based on the DLD and DLST. UM patients were categorised into low- and high-risk groups based on the median risk score, as follows:

$$\text{Risk score} = \text{expression (DLD)} \times \text{coefficient (DLD)} + \text{expression (DLST)} \times \text{coefficient (DLST)}$$

2.3. Clinical information analysis

Via "survminer" R package, Kaplan-Meier curves were generated to analyse differences of OS between the high- and low-risk groups. Applying ‘timeROC’ R package, Receiver operating characteristic (ROC) curves were used to assess the forecast accuracy of the prognostic signature.

2.4. Immune-related analysis

To analyse immunological differences, ssGSEA was used to identify the degree of infiltration of 23 types of immune cells in tumours between the high- and low-risk groups. Applying the R package “ggplot2” and “ggpubr”, immune checkpoints analysis was conducted ($P < 0.05$).

2.5. Drug sensitivity

The R package 'gpubr' and 'pRRophetic' R packages were used by us to explore chemotherapeutic drugs in different risk groups of UM patients by calculating the half maximum inhibitory concentration (IC50) values of different drugs.

2.6. Cells

The human choroidal melanoma cell line, OCM-1, was obtained from the Sun Yat-sen Eye Center of Sun Yat-sen University. The human retinal pigment epithelial cell line ARPE-19 was purchased from ATCC. All cells were maintained in Dulbecco's modified Eagle's medium (DMEM)/F12 medium nutrient Mixture F-12 (Ham's) (1:1) with L-Glutamine and Sodium Pyruvate, with Hepes 15 mM DMEM: F12 (1:1) supplemented with 10 % foetal bovine serum (FBS; Gibco, Rockville, MD, USA) and 100 U/mL penicillin-streptomycin mixture (Gibco, USA) at 37 °C in 5 % CO_2.

2.7. RNA extraction and qPCR

RNA-easy Isolation Reagent (R701, Vazyme, China) was used to extract total RNA from OCM-1 and ARPE-19 cells. The cDNA of

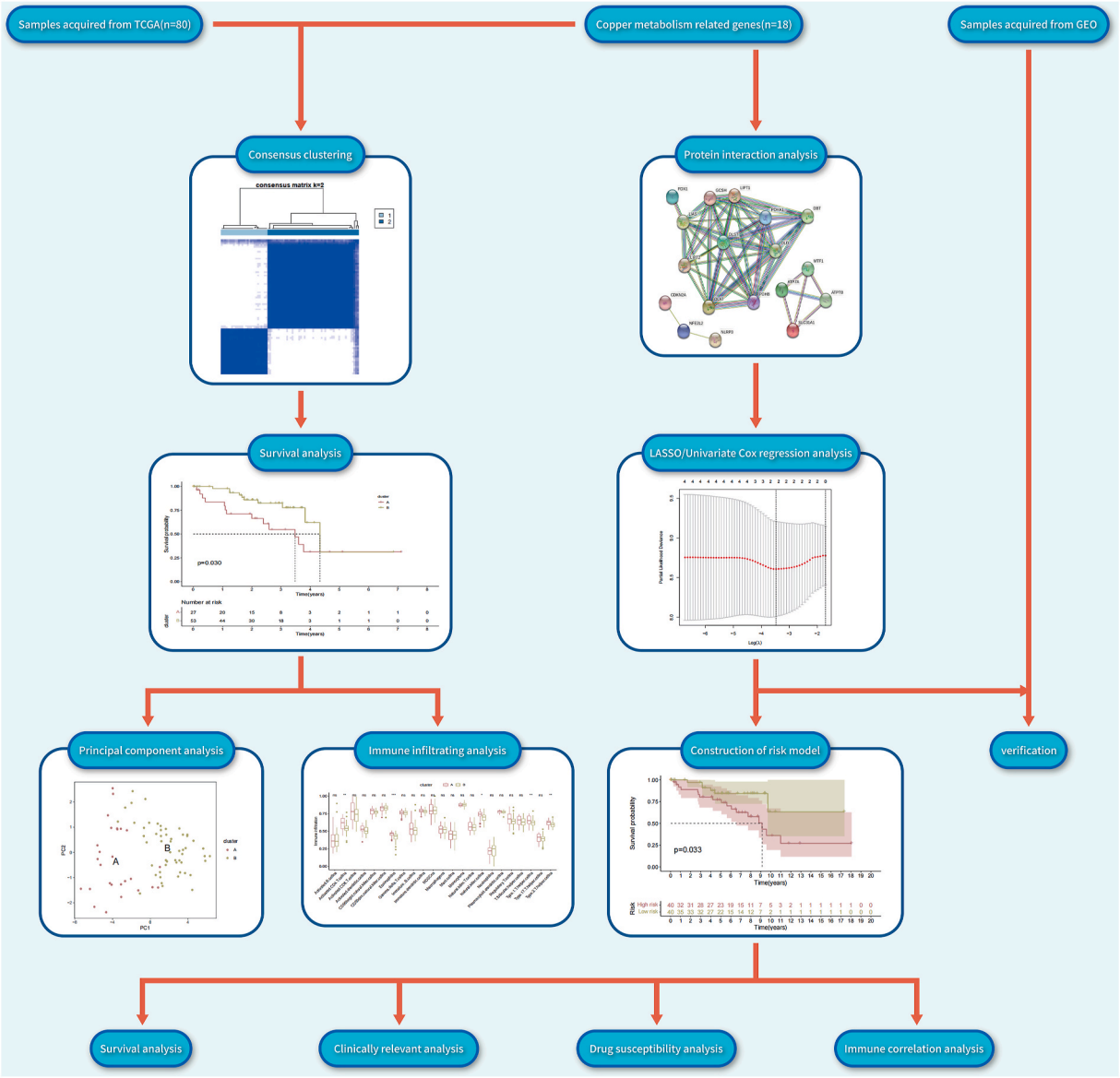

Fig. 1. Flow chart illustrating the study rationale and design.

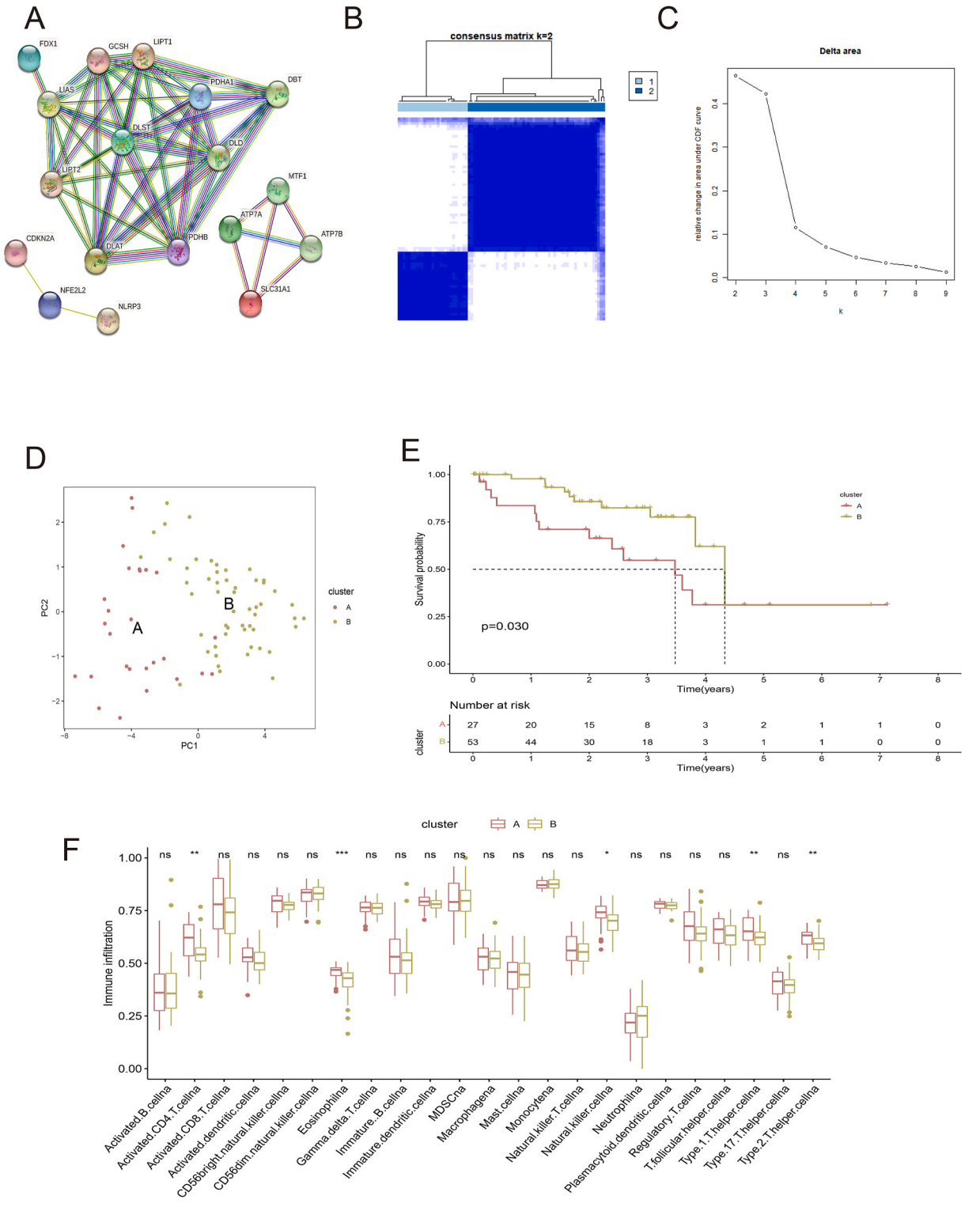

Fig. 2. Constructing cuproptosis-related molecular subtypes. (A) Construction of a protein-protein interaction (PPI) network revealed the interaction of cuproptosis-related genes. (B, C) Unsupervised clustering of the 18 cuproptosis-related genes in uveal melanoma (UM) and k = 2 was selected. (D) Principal Component Analysis (PCA) of two cuproptosis-related molecular subtypes. (E) The overall survival of the UM cohort, as identified from data in The Cancer Genome Atlas (TCGA), with two cuproptosis-related molecular subtypes. (F) Immune cells infiltration degree of two cuproptosis-related molecular subtypes.

ARPE-19 and OCM-1 cells were obtained using an RT Reagent kit (Thermo Fisher). GAPDH was chosen as an internal reference for normalization. The following primers were purchased from Shanghai Sangong Biotechnology (Shanghai, China):

DLD-Forward primer: 5'-GTCGTGTGTACTGCTCCTTGGC-3';
DLD-Reverse primer: 5'-AATCGGCTGATCTGCGTAAGTTCTC-3'.
DLST-Forward primer: 5'-AGGGAGATGTCAGGTGGGAGAAAG-3';
DLST-Reverse primer: 5'-AAAGAGCTTCAATCACGCCATTTGC-3'.

2.8. Protein extraction and western blot

ARPE-19 and UM cells were seeded into culture dishes at the sixth generation, lysed with RIPA buffer containing a protease inhibitor, and centrifuged to obtain the supernatant. The Pierce BCA Protein Assay Kit (Thermo Fisher Scientific, Waltham, MA, USA)

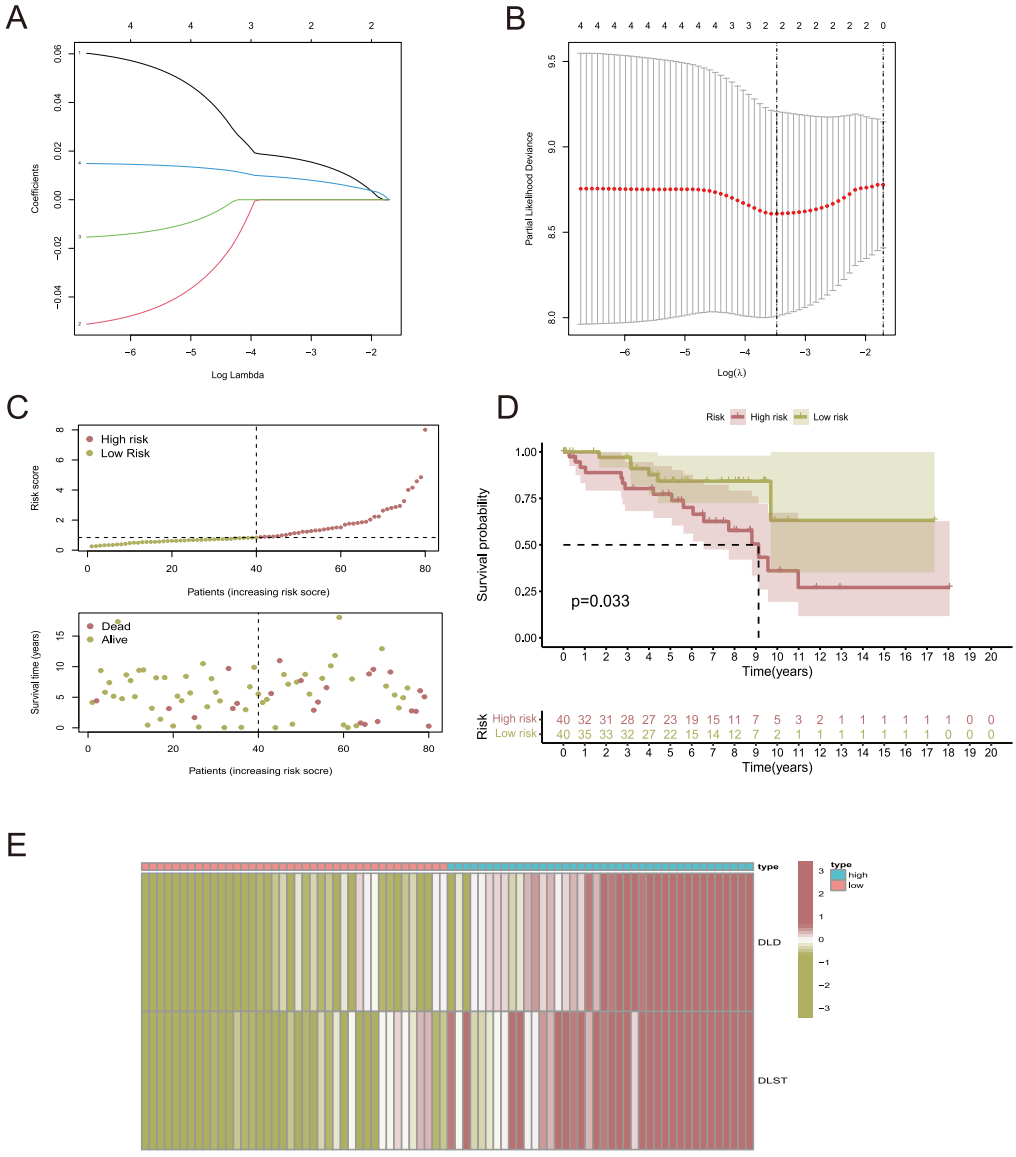

Fig. 3. Establishing the cuproptosis-related prognostic signature for UM patients. (A, B) Cvfit and lambda curves of the LASSO regression. (C) Risk score and survival status of the two risk groups. (D) Overall survival of TCGA-UM cohort with the two risk groups. (E) Distribution of DLD and DLST in two risk groups.

was used to measure protein concentration. After being blocked, the polyvinylidene difluoride filter (PVDF) membranes were incubated with primary antibodies overnight at 4 °C. The next day, the PVDF membranes were incubated with horseradish peroxidase-conjugated secondary antibodies (1:2000) for 2 h. Blots were imaged using an enhanced chemiluminescence system (Biosharp) [17]. DLD antibodies were purchased from Proteintech (China), and other antibodies were purchased from Servicebio (China). All the data were analysed using GraphPad Prism (version 9.5.1) software.

2.9. Statistical analysis

The data is dealt with GraphPad Prism software and expressed as mean ± SD. $P < 0.05$ was considered to have statistical significance. The R 4.2.0 was applied for data processing.

3. Results

3.1. Identification and correlation analysis of two molecular subtypes based on cuproptosis-related genes

The data analysis process is illustrated in Fig. 1. Based on the previous literature on cuproptosis, 18 genes related to cuproptosis were screened. The correlation between these genes was determined based on a protein interaction analysis diagram using the STRING database (Fig. 2A). Subsequently, a consensus cluster analysis of 80 uveal melanoma samples from the TCGA-UVM cohort according to different cuproptosis-related gene expression patterns was performed (Fig. 2B and C). Among $k = 2$ to $k = 9$, $k = 2$ was chosen, and patients were split into two cuproptosis-related molecular subtypes, called CRD clusters A and B. Principal component analysis (PCA) was used to visualise the distribution of CRD clusters based on the genomic expression in UM patients (Fig. 2D). Survival analysis revealed that the total survival period of patients with CRD cluster B was significantly better than that of patients with CRD cluster A ($p < 0.05$) (Fig. 2E). Increasing evidence has shown that the degree of cancer malignancy is closely associated with the tumour immune microenvironment [18]. Owing to the significant difference in OS between the two groups of patients with UM, we conducted an immune correlation analysis for the different groups. Statistical analysis showed that the numbers of activated CD4T cells, eosinophils, natural killer cells, type 1 T helper cells, and type 2 T helper cells in CRD cluster A were significantly higher than those in CRD cluster B (Fig. 2 F). These results indicate that the survival time and immune status of the two molecular subtypes are significantly different, and that the enrichment of different immune cells may affect the overall survival time of UM patients.

3.2. Construction of cuproptosis-related prognostic signature for UM patients

We constructed a prognostic signature to assess the prognostic value of cuproptosis-related genes in uveal melanoma. Through univariate COX regression analysis, four genes related to the prognosis of uveal melanoma were screened out from 18 cuproptosis-related genes (Fig. 3A). LASSO regression analysis was then carried out to identify the cuproptosis-related genes with prognostic value through dimension reduction, and the relative coefficient of genes was computed (Fig. 3B and C). Lastly, two optimal genes DLD and DLST were selected to construct a prognosis model. The coefficients of DLD and DLST were listed in Table 1. The UM risk scores were calculated using a formula which included the expression of DLD and DLST and the coefficients: risk score = exp(DLD) × coef (DLD) + exp(DLST) × coef(DLST). Based on the median value, the established prognostic model successfully divided patients with uveal melanoma into high- and low-risk groups. The survival status and risk score distribution of the patients are shown in Fig. 3D. The results of the survival analysis showed that patients in the high-risk group had poor prognosis (Fig. 3E). The heat map in Fig. 3F illustrates the expression trends of DLD and DLST in the two risk groups.

3.3. Assessment of correlation between cuproptosis-related prognostic signature and clinical characteristics

We further analysed the correlation between the risk scoring model and common clinical characteristics. The results of the univariate Cox analysis showed that the risk score was significantly related to overall survival by univariate Cox analysis (Fig. 4A), and multivariate analysis showed that this cuproptosis-related risk score was an independent prognostic factor for patients with uveal melanoma (Fig. 4B). The ROC curve shows acceptable evaluation results. Time-dependent ROC analysis shows that the built risk model can accurately predict over a 3-yr period. The area under the ROC curve (AUC) of 1, 2 and 3 yr is 0.862, 0.749 and 0.809, respectively (Fig. 4C). In Fig. 4D, the correlation between the expression levels of the two key genes and the clinical indicators is presented as heat maps.

Table 1
Coefficients of DLD and DLST.

id	coef
DLD	0.021067135
DLST	0.01146033

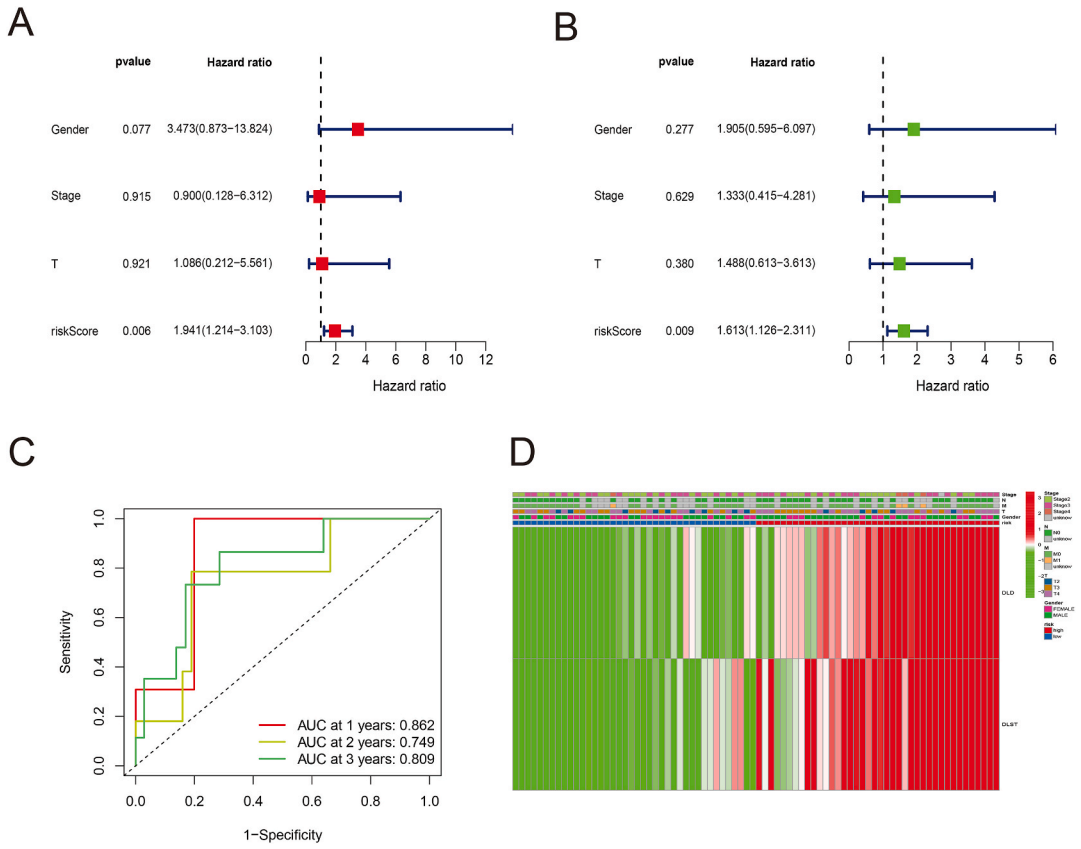

Fig. 4. Assessment of correlation between the prognostic signature and clinical characteristics. (A) Univariate and (B) multivariate Cox regression analysis of clinical characteristics. (C) The time dependent ROC analysis. (D) Heatmap visualizing clinical characteristics, expression of two prognostic cuproptosis-related genes and risk group of each UM patient. (E, F) Waterfall plots of TMB information in two risk groups.

3.4. Immune microenvironment of the cuproptosis-related prognostic signature

Increasing evidence has shown that the degree of cancer malignancy is related to the tumour immune microenvironment. Considering the significant difference in prognosis between the two groups of patients with uveal melanoma, we speculate that the tumor immune microenvironment plays a notable role in the progression of uveal melanoma. We then performed an immune correlation analysis. First, we analysed the immune cells of different risk groups and drew a heat map (Fig. 5A). Immune function analysis was performed (Fig. 5B). To further investigate the differences in the immune cell infiltration microenvironments between the two risk groups, the infiltration levels of 23 common immune cell types were evaluated using ssGSEA (Fig. 5C). The results showed that the two clusters exhibited significantly different immune cell infiltration characteristics. Activated CD4 + T cells, CD8 + T cells, eosinophils, and natural killer cells showed higher infiltration levels in the high-risk group. Subsequently, we analysed the immune checkpoints and studied the expression of genes related to these checkpoints. As shown in the figure, most immune checkpoint-related genes, such as CD27 and IDO1, showed higher expression levels in the high-risk groups (Fig. 5D). In summary, there was a significant immune difference between the two high-risk groups, and the high expression of immune checkpoints in high-risk groups suggests significant immunotherapy potential.

3.5. Analysis of potential drugs targeting the cuproptosis-related prognostic signature

Using drug sensitivity analysis, potential drugs targeting cuproptosis metabolism for UM patients were screened by us (Fig. 6A–H). We evaluated the treatment results according to the half-maximum inhibitory concentration (IC50) for each UM patient, based on PRROPHIC algorithm. Eight types of drugs were identified and IC50 levels of the two risk groups were compared. A-770041, CGP-60474, CGP-082996, cycloamine, dasatinib, paclitaxe, and rapamycin showed higher sensitivities in the low-risk group. Interestingly, UM patients in the high-risk group are more sensitive to erlotinib, which may be a novel therapeutic drug for UM patients. In general, based on drug sensitivity analysis, UM patients in the low-risk group have been proven to have better drug sensitivity than those in the high-risk group, which further proves that the low-risk group had better prognosis and the reliability of the cuproptosis-related prognostic signature as a biomarker. These results are a strong indication that erlotinib is a candidate therapy for patients in the high-risk category. Additionally, several newly discovered drugs can be used as potential drugs for to treat uveal melanoma.

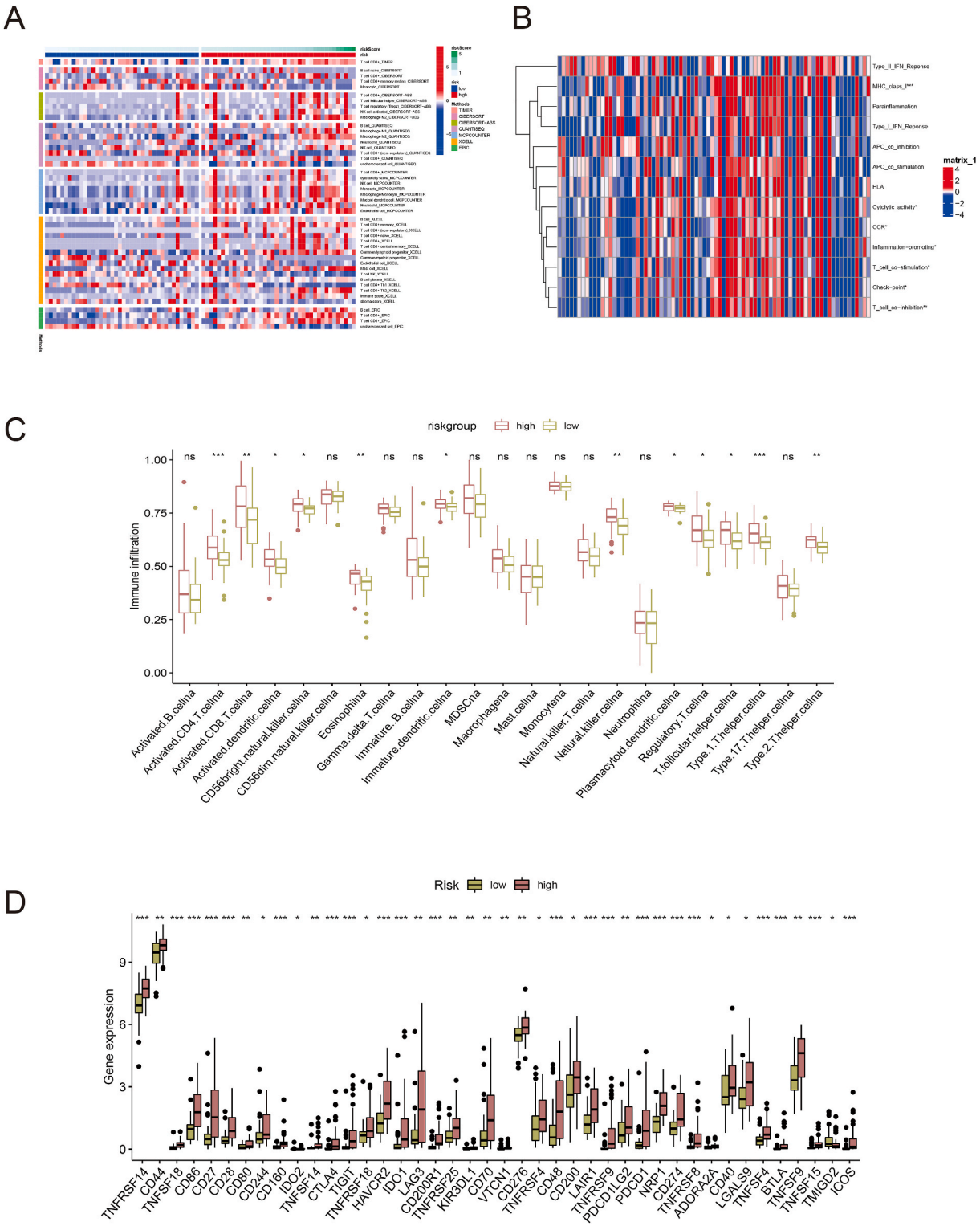

Fig. 5. Immune-related analysis of two risk groups. (A) The heatmap of immune microenvironment of UM patients in low- and high-risk groups. (B) Immunological function analysis of two risk groups. (C) Boxplot of the 23 immune cells infiltration degree of two risk groups. (D) Analysis of differences in immune checkpoints between two risk groups.

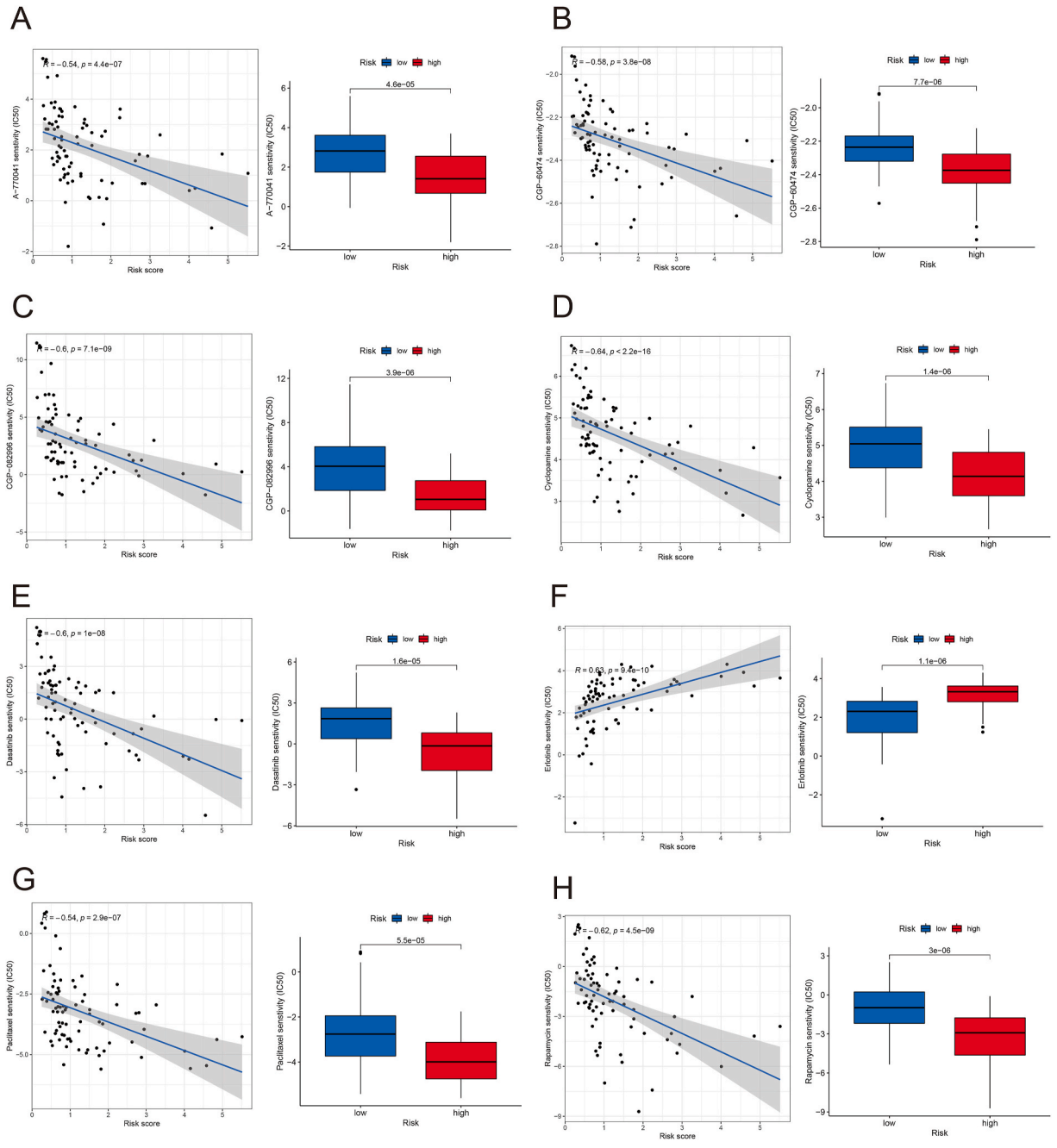

Fig. 6. Drug sensitivity analysis.

3.6. In the validation cohort, the risk model for uveal melanoma was associated with time and prognosis

We further validated the established prognostic risk-scoring model in the validation queue of GSE22138. Based on the previously obtained data, patients with UM in the validation queue were divided into high- and low-risk groups (Fig. 7A). After survival analysis, it was found that this model was meaningful in the geo database. Expression of the two candidate genes is shown as a heat map (Fig. 7B). Survival analysis confirmed that the prognosis of patients in the high-risk group was poor (Fig. 7C). These results indicate that in the validation cohort, the established prognostic signature was related to the time and prognosis of uveal melanoma.

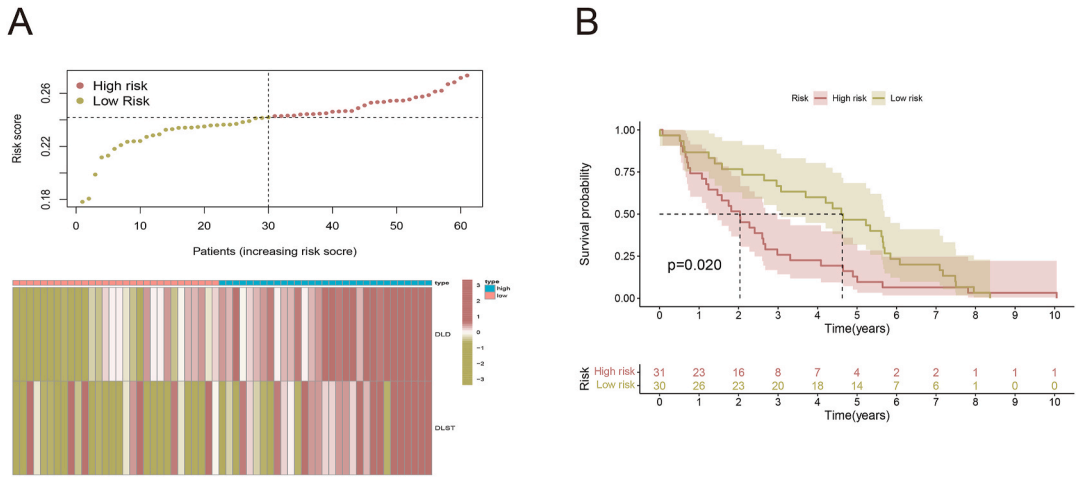

Fig. 7. Validation of the cuproptosis-related prognostic signature by the GSE22138. (A) Distribution of risk score and survival status of UM patients in the GSE22138. (B) Overall survival of the two risk groups in the GSE22138.

3.7. Experimental verification of high expression of DLD and DLST in UM cell lines

To verify the identified prognostic cuproptosis-related genes, the expression levels of DLD and DLST in UM were validated through in vitro experiments. To verify the mRNA expression levels, we used qPCR to verify the differences between DLD and DLST in the UM cell line OCM-1 and the human spontaneously arising retinal pigment epithelia (RPE) cell line ARPE-19. As shown in Fig. 8A and B, consistent with the results of the bioinformatics analysis, both DLD and DLST were highly expressed in OCM-1 cells. Western blotting experiments were conducted to investigate the protein expression levels of DLD and DLST in UM cell lines. Consistent with the qPCR

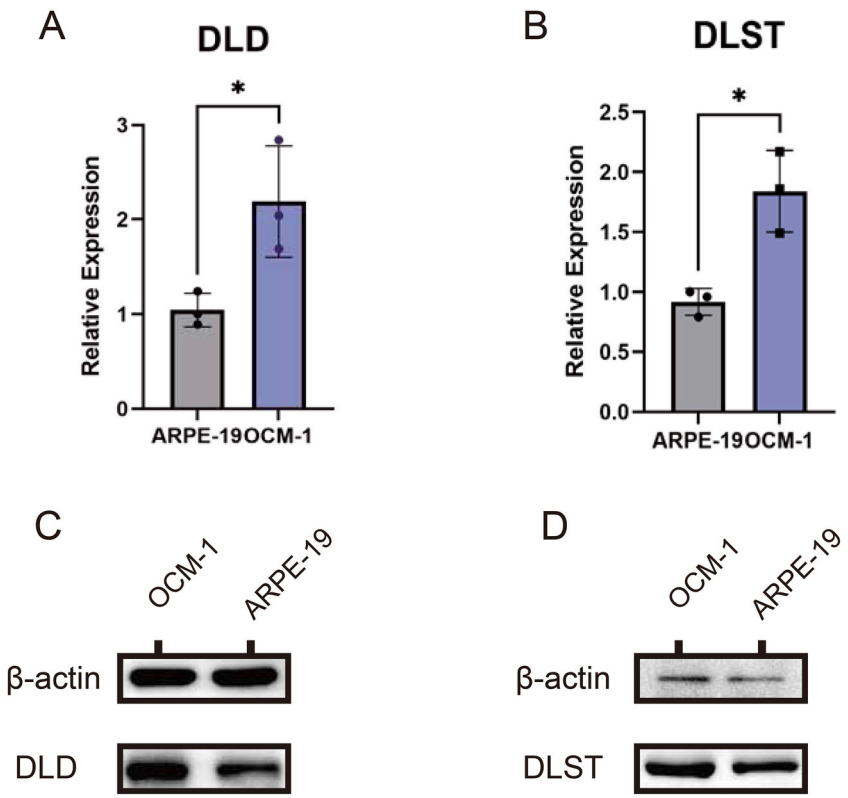

Fig. 8. Experimental verification of DLD and DLST in UM cell lines. (A, B) qPCR result showed that DLD and DLST had high expression in UM cell line OCM-1 compared normal human retinal epithelial cell ARPE-19. (C, D) WB detection of DLD and DLST expression in UM cell line OCM-1. The data are presented as the means ± SEMs. *P < 0.05, **P < 0.01, ***P < 0.001. The experiments were repeated three times.

results, DLD and DLST showed significant high expression in OCM-1 cells. We verified the accuracy of our previous analysis through in vitro experiments.

4. Discussion

Uveal melanoma is considered the primary (highest incidence) intraocular malignant tumour, and the mortality rate is as high as 50 % in patients [19,20]. Currently, UM diagnosis is primarily based on clinical evaluations such as ophthalmoscopy, biomicroscopy, and ultrasonography. In addition, magnetic resonance imaging (MRI) plays an important role in confirming the diagnosis, assessing the local extent of UM and its impact on UM treatment decisions, and follow-up after radiotherapy [21]. The main goal of UM treatment for UM is to protect the eye and its visual function, and prevent tumour metastasis [22]. Radiotherapy is more popular than enucleation therapy. Close-range radiation therapy for plaques is the most commonly used eye protection therapy and is suitable for small- and medium-sized uveal melanomas. Enucleation surgery is suitable for treating advanced melanoma and eye pain caused by complications [22]. Nevertheless, the prognosis of UM remains poor. Therefore, researchers are searching for new biomarkers that can improve the prognosis of patients with UM. The expression of ABCB5 is associated with faster metastatic progression and poorer prognosis, indicating its role as a prognostic factor in uveal melanoma [23]. The expression of TAP1 is positively correlated with clinical pathological factors and poor prognosis of UM and can serve as a new therapeutic target for UM patients [24]. In a study based on 85 cases of primary UM, the authors reported a statistically significant correlation between PRAME expression and higher metastasis risk and lower metastasis-free survival in patients with UM [25]. Studies have also shown that lactate metabolism may be a prognostic marker of UM progression and a potential therapeutic target [26]. Therefore, it is necessary to analyse the clinical characteristics, overall survival rate, immune microenvironment, and drug sensitivity of patients with UM to provide guidance for early clinical diagnosis and prognostic prediction.

Cuproptosis was first discovered by Tsvetkov et al. as a novel form of regulatory cell death (RCD) [27]. Recently, researchers have used these cuproptosis-related genes for bioinformatic analysis and have constructed prognostic signatures in many cancers, which have demonstrated good predictive ability for prognosis [28–30]. However, no study has constructed a prognostic signature based on cuproptosis-related genes in UM. Therefore, constructing a cuproptosis-related prognostic signature of UM and a probe for its function is a valuable contribution to the literature on this topic [27,31].

In this study, based on mechanism of cuproptosis documented by Tsvetkov et al. we identified 18 cuproptosis-related genes. On the basis of expression of 18 cuproptosis-related genes, patients with UM were divided into two CRD clusters using consensus clustering. The two CRDclusters showed significant differences in survival and immune cell infiltration. Upon applying Lasso Cox regression, DLD and DLST was identified as prognostic cuproptosis-related genes to constructing prognostic signature. By calculating the risk score, the samples were classified into high-and low-risk groups. Patients in high-risk group exhibited worse outcomes. The ROC curve is considered a reliable tool for predicting cancer prognosis [32]. This cuproptosis-related prognostic signature showed an accurately predicting prognostic value in UM according to Cox regression analysis and ROC curve confirmed the predictive accuracy. Immune function analysis revealed that patients in the high-risk group were enriched in the inflammation-promoting T-cell co-inhibition pathway and MHC class I. Recent research has found that inflammation and cancer are inseparable and that the biological processes associated with inflammation affect all stages of cancer development and treatment [33]. ssGSEA was also used to analyse the immune cell infiltration abundance, and it was found that patients in the high-risk group had a higher level of immune cell infiltration. To date, several treatments targeting patients with UM have yielded disappointing clinical results. A significant connection between the cuproptosis-related risk signature and immunotherapy was found, which indicated this signature provides new possibilities for HRG patients to provide more effective immunotherapy strategies. To provide guidance for clinical treatment, we conducted immune checkpoint analysis and drug screening using IC50 analysis. Therefore, erlotinib can be used as a therapeutic drug for high-risk patients with UM. As an EGFR-targeted drug, erlotinib not only plays a role in non-small cell lung cancer, but also has activity in head and neck tumours, glioblastoma, and other tumour types. In the present study, we found that erlotinib may also affect UM. The prognostic accuracy of this signature was validated in the independent cohorts-GSE22138 from the Gene Expression Omnibus (GEO) database.

Dihydrolipoamide dehydrogenase (DLD) is an enzyme that produces reactive oxygen species related to its redox activity [34]. The results of pan-cancer analysis showed that the DLD gene is highly expressed in colon, liver, lung, gastric, kidney, endometrial, and ovarian cancers [35]. As a component of the α-ketoglutarate dehydrogenase complex, dihydrolipoamide S-succinyltransferase (DLST) regulates glutamine metabolism in the tricarboxylic acid (TCA) cycle [36]. High DLST expression is often associated with poor prognosis in tumours [37]. However, there is no experimental evidence demonstrating the roles of DLD and DLST in UM. In this study, we validated the high expression of DLD and DLST in UM cells through qPCR and Western blot experiments.

This study also has some limitations. Firstly, due to the limited number of UM samples, more UM samples are need to test the stability of the cuproptosis-related prognostic signature. Further research is required to demonstrate the roles of DLD and DLST in UM.

5. Conclusion

In this study, we constructed a gene signature based on cuproptosis-related genes as a promising tool for uveal melanoma stratification. It is a prognostic classifier that can assist in individualised clinical prediction and treatment and in making clinical decisions.

Data availability statement

Data for this study can be obtained by contacting the corresponding author upon reasonable request.

The data used in this study are all available from the TCGA database (https://portal.gdc.cancer.gov/) and GEO database (https://www.ncbi.nlm.nih.gov/geo/).

Funding

Postgraduate Research & Practice Innovation Program of Jiangsu Province (134422631103).

Ethics approval and consent to participate

Not applicable.

Code availability

Not applicable.

Consent for publication

Not applicable.

CRediT authorship contribution statement

Ying Yang: Writing – review & editing, Writing – original draft, Validation, Formal analysis, Data curation. **Qixuan Li:** Writing – review & editing, Writing – original draft, Methodology, Formal analysis. **Jia Chen:** Writing – review & editing, Methodology, Data curation. **Yangchen Guo:** Writing – review & editing, Software. **Yu Cai:** Writing – review & editing, Project administration. **Wenmin Zhao:** Writing – review & editing, Resources. **Shu Su:** Writing – review & editing, Conceptualization. **Aimin Sang:** Writing – review & editing, Funding acquisition, Conceptualization.

Declaration of competing interest

The authors declare the following financial interests/personal relationships which may be considered as potential competing interests:Aimin Sang reports financial support was provided by Postgraduate Research & Practice Innovation Program of Jiangsu Province. If there are other authors, they declare that they have no known competing financial interests or personal relationships that could have appeared to influence the work reported in this paper.

Acknowledgements

The original images of western blotting have been put into supplement file 1.

Appendix A. Supplementary data

Supplementary data to this article can be found online at https://doi.org/10.1016/j.heliyon.2024.e36324.

References

[1] C. Chattopadhyay, D.W. Kim, D.S. Gombos, J. Oba, Y. Qin, M.D. Williams, B. Esmaeli, E.A. Grimm, J.A. Wargo, S.E. Woodman, et al., Uveal melanoma: from diagnosis to treatment and the science in between, Cancer 122 (15) (2016) 2299–2312.
[2] C. Chattopadhyay, D.W. Kim, D.S. Gombos, J. Oba, Y. Qin, M.D. Williams, B. Esmaeli, E.A. Grimm, J.A. Wargo, S.E. Woodman, et al., Uveal melanoma: from diagnosis to treatment and the science in between, Cancer 122 (15) (2016) 2299–2312.
[3] K.N. Smit, M.J. Jager, A. de Klein, E. Kiliç, Uveal melanoma: towards a molecular understanding, Prog. Retin. Eye Res. 75 (2020) 100800.
[4] S. Kaliki, C.L. Shields, Uveal melanoma: relatively rare but deadly cancer, Eye (Lond) 31 (2) (2017) 241–257.
[5] S. Kaliki, C.L. Shields, J.A. Shields, Uveal melanoma: estimating prognosis, Indian J. Ophthalmol. 63 (2) (2015).
[6] A.D. Singh, M.E. Turell, A.K. Topham, Uveal melanoma: trends in incidence, treatment, and survival, Ophthalmology 118 (9) (2011) 1881–1885.
[7] M. Arredondo, M.T. Nunez, Iron and copper metabolism, Mol. Aspect. Med. 26 (4–5) (2005) 313–327.
[8] E.J. Ge, A.I. Bush, A. Casini, P.A. Cobine, J.R. Cross, G.M. DeNicola, Q.P. Dou, K.J. Franz, V.M. Gohil, S. Gupta, et al., Connecting copper and cancer: from transition metal signalling to metalloplasia, Nat. Rev. Cancer 22 (2) (2022) 102–113.
[9] P. Tsvetkov, S. Coy, B. Petrova, M. Dreishpoon, A. Verma, M. Abdusamad, J. Rossen, L. Joesch-Cohen, R. Humeidi, R.D. Spangler, et al., Copper induces cell death by targeting lipoylated TCA cycle proteins, Science 375 (6586) (2022) 1254–1261.
[10] J.-Q. Chen, J. Russo, Dysregulation of glucose transport, glycolysis, TCA cycle and glutaminolysis by oncogenes and tumor suppressors in cancer cells, Biochim. Biophys. Acta 1826 (2) (2012) 370–384.
[11] B.J. Altman, Z.E. Stine, C.V. Dang, From Krebs to clinic: glutamine metabolism to cancer therapy, Nat. Rev. Cancer 16 (10) (2016) 619–634.
[12] Y. Ding, J. Yu, X. Chen, S. Wang, Z. Tu, G. Shen, H. Wang, R. Jia, S. Ge, J. Ruan, et al., Dose-dependent carbon-dot-induced ROS promote uveal melanoma cell tumorigenicity via activation of mTOR signaling and glutamine metabolism, Adv. Sci. 8 (8) (2021) 2002404.
[13] S.-R. Li, L.-L. Bu, L. Cai, Cuproptosis: lipoylated TCA cycle proteins-mediated novel cell death pathway, Signal Transduct. Targeted Ther. 7 (1) (2022) 158.

[14] S. Xu, D. Liu, T. Chang, X. Wen, S. Ma, G. Sun, L. Wang, S. Chen, Y. Xu, H. Zhang, Cuproptosis-associated lncRNA establishes new prognostic profile and predicts immunotherapy response in clear cell renal cell carcinoma, Front. Genet. 13 (2022) 938259.
[15] Z. Zhang, X. Zeng, Y. Wu, Y. Liu, X. Zhang, Z. Song, Cuproptosis-related risk score predicts prognosis and characterizes the tumor microenvironment in hepatocellular carcinoma, Front. Immunol. 13 (2022) 925618.
[16] Q. Li, T. Wang, J. Zhu, A. Zhang, A. Wu, Y. Zhou, J. Shi, A cuproptosis-related lncRNAs risk model to predict prognosis and guide immunotherapy for lung adenocarcinoma, Ann. Transl. Med. 11 (5) (2023) 198.
[17] Y. Xu, K. Cui, J. Li, X. Tang, J. Lin, X. Lu, R. Huang, B. Yang, Y. Shi, D. Ye, et al., Melatonin attenuates choroidal neovascularization by regulating macrophage/microglia polarization via inhibition of RhoA/ROCK signaling pathway, J. Pineal Res. 69 (1) (2020) e12660.
[18] W. Li, Y. Deng, Q. Chu, PJCl Zhang, Gut Microbiome and Cancer Immunotherapy, vol. 447, 2019, pp. 41–47.
[19] A.D. Singh, M.E. Turell, A.K. Topham, Uveal melanoma: trends in incidence, treatment, and survival, Ophthalmology 118 (9) (2011) 1881–1885.
[20] M.J. Jager, C.L. Shields, C.M. Cebulla, M.H. Abdel-Rahman, H.E. Grossniklaus, M.H. Stern, R.D. Carvajal, R.N. Belfort, R. Jia, J.A. Shields, et al., Uveal melanoma, Nat. Rev. Dis. Prim. 6 (1) (2020) 24.
[21] P. Foti, M. Travali, R. Farina, S. Palmucci, C. Spatola, L. Raffaele, V. Salamone, R. Caltabiano, G. Broggi, L. Puzzo, et al., Diagnostic methods and therapeutic options of uveal melanoma with emphasis on MR imaging-Part I: MR imaging with pathologic correlation and technical considerations, Insights into imaging 12 (1) (2021) 66.
[22] P. Foti, M. Travali, R. Farina, S. Palmucci, C. Spatola, R. Liardo, R. Milazzotto, L. Raffaele, V. Salamone, R. Caltabiano, et al., Diagnostic methods and therapeutic options of uveal melanoma with emphasis on MR imaging-Part II: treatment indications and complications, Insights into imaging 12 (1) (2021) 67.
[23] G. Broggi, G. Musumeci, L. Puzzo, A. Russo, M. Reibaldi, M. Ragusa, A. Longo, R. Caltabiano, Immunohistochemical expression of ABCB5 as a potential prognostic factor in uveal melanoma, Appl. Sci. 9 (7) (2019) 1316.
[24] R. Zhu, Y. Chen, B. Wang, Y. You, X. Wang, H. Xie, F. Jiang, M. Zhang, TAP1, a potential immune-related prognosis biomarker with functional significance in uveal melanoma, BMC Cancer 23 (1) (2023) 146.
[25] G. Broggi, M. Failla, A. Russo, A. Longo, A. Palicelli, M. Zanelli, C. Lombardo, C. Loreto, F. Merolla, R. Di Crescenzo, et al., Immunohistochemical expression of PRAME is a marker of poor prognosis in uveal melanoma: a clinico-pathologic and immunohistochemical study on a series of 85 cases, Pathol. Res. Pract. 247 (2023) 154543.
[26] L. Longhitano, S. Giallongo, L. Orlando, G. Broggi, A. Longo, A. Russo, R. Caltabiano, C. Giallongo, I. Barbagallo, M. Di Rosa, et al., Lactate rewrites the metabolic reprogramming of uveal melanoma cells and induces quiescence phenotype, Int. J. Mol. Sci. 24 (1) (2023) 24.
[27] P. Tsvetkov, S. Coy, B. Petrova, M. Dreishpoon, A. Verma, M. Abdusamad, J. Rossen, L. Joesch-Cohen, R. Humeidi, R.D. Spangler, et al., Copper induces cell death by targeting lipoylated TCA cycle proteins, Science 375 (6586) (2022) 1254–1261.
[28] H. Lv, X. Liu, X. Zeng, Y. Liu, C. Zhang, Q. Zhang, J. Xu, Comprehensive analysis of cuproptosis-related genes in immune infiltration and prognosis in melanoma, Front. Pharmacol. 13 (2022) 930041.
[29] Z. Bian, R. Fan, L. Xie, A novel cuproptosis-related prognostic gene signature and validation of differential expression in clear cell renal cell carcinoma, Genes 13 (5) (2022).
[30] S. Song, M. Zhang, P. Xie, S. Wang, Y. Wang, Comprehensive analysis of cuproptosis-related genes and tumor microenvironment infiltration characterization in breast cancer, Front. Immunol. 13 (2022) 978909.
[31] Q. Li, T. Wang, Y. Zhou, J. Shi, Cuproptosis in lung cancer: mechanisms and therapeutic potential, Mol. Cell. Biochem. 479 (6) (2024) 1487–1499.
[32] J.N. Mandrekar, Receiver operating characteristic curve in diagnostic test assessment, J. Thorac. Oncol. 5 (9) (2010) 1315–1316.
[33] J. Hou, M. Karin, B. Sun, Targeting cancer-promoting inflammation - have anti-inflammatory therapies come of age? Nat. Rev. Clin. Oncol. 18 (5) (2021) 261–279.
[34] D. Shin, J. Lee, J.H. You, D. Kim, J.L. Roh, Dihydrolipoamide dehydrogenase regulates cystine deprivation-induced ferroptosis in head and neck cancer, Redox Biol. 30 (2020) 101418.
[35] H. Qi, D. Zhu, Oncogenic role of copper-induced cell death-associated protein DLD in human cancer: a pan-cancer analysis and experimental verification, Oncol. Lett. 25 (5) (2023) 214.
[36] N.M. Anderson, X. Qin, J.M. Finan, A. Lam, J. Athoe, R. Missiaen, N. Skuli, A. Kennedy, A.S. Saini, T. Tao, et al., Metabolic enzyme DLST promotes tumor aggression and reveals a vulnerability to OXPHOS inhibition in high-risk neuroblastoma, Cancer Res. 81 (17) (2021) 4417–4430.
[37] N. Shen, S. Korm, T. Karantanos, D. Li, X. Zhang, E. Ritou, H. Xu, A. Lam, J. English, W.X. Zong, et al., DLST-dependence dictates metabolic heterogeneity in TCA-cycle usage among triple-negative breast cancer, Commun. Biol. 4 (1) (2021) 1289.